

Standoff detection via single-beam spectral notch filtered pulses

Adi Natan, Jonathan M. Levitt, Leigh Graham, Ori Katz, and Yaron Silberberg

Citation: *Appl. Phys. Lett.* **100**, 051111 (2012); doi: 10.1063/1.3681365

View online: <http://dx.doi.org/10.1063/1.3681365>

View Table of Contents: <http://apl.aip.org/resource/1/APPLAB/v100/i5>

Published by the [American Institute of Physics](#).

Related Articles

A two-color tunable infrared/vacuum ultraviolet spectrometer for high-resolution spectroscopy of molecules in molecular beams

Rev. Sci. Instrum. **83**, 014102 (2012)

Fast magneto-optical spectrometry by spectrometer

Rev. Sci. Instrum. **83**, 013103 (2012)

High resolution far-infrared Fourier transform spectroscopy of radicals at the AILES beamline of SOLEIL synchrotron facility

Rev. Sci. Instrum. **82**, 113106 (2011)

Tunable excitation source for coherent Raman spectroscopy based on a single fiber laser

Appl. Phys. Lett. **99**, 181112 (2011)

Characterization of near-terahertz complementary metal-oxide semiconductor circuits using a Fourier-transform interferometer

Rev. Sci. Instrum. **82**, 103106 (2011)

Additional information on *Appl. Phys. Lett.*

Journal Homepage: <http://apl.aip.org/>

Journal Information: http://apl.aip.org/about/about_the_journal

Top downloads: http://apl.aip.org/features/most_downloaded

Information for Authors: <http://apl.aip.org/authors>

ADVERTISEMENT



LakeShore Model 8404 developed with **TOYO Corporation**
NEW AC/DC Hall Effect System Measure mobilities down to 0.001 cm²/V s

Standoff detection via single-beam spectral notch filtered pulses

Adi Natan,^{a)} Jonathan M. Levitt, Leigh Graham, Ori Katz, and Yaron Silberberg
Department of Complex Systems, Weizmann Institute of Science, Rehovot 76100, Israel

(Received 22 November 2011; accepted 13 January 2012; published online 3 February 2012)

We demonstrate single-beam coherent anti-Stokes Raman spectroscopy (CARS), for detecting and identifying traces of solids, including minute amounts of explosives, from a standoff distance (>50 m) using intense femtosecond pulses. Until now, single-beam CARS methods relied on pulse-shapers in order to obtain vibrational spectra. Here, we present a simple and easy-to-implement detection scheme, using a commercially available notch filter that does not require the use of a pulse-shaper. © 2012 American Institute of Physics. [doi:10.1063/1.3681365]

Laser based remote detection and identification of hazardous materials, including biological warfare agents and explosives have recently been the focus of intense research efforts.^{1–7} In particular, it has been shown that the vibrational response of molecules provides a unique fingerprint for various molecular species and, hence, vibrational spectra can be used for identification.^{5–11} One such suitable technique for identifying vibrational spectra is coherent anti-Stokes Raman spectroscopy (CARS).¹² In CARS, pump ω_p and Stokes ω_s photons excite a vibrational level ω_{vib} that is subsequently probed with a probe photon ω_{pr} . The vibrational levels are resolved by measuring the scattered anti-Stokes photons located at $\omega_{vib} + \omega_{pr} = \omega_{AS}$, and coherent signal buildup occurs when $k_p - k_s + k_{pr} - k_{AS} = 0$. In conventional CARS, narrowband (ps) pump and probe beams are tuned such that $\omega_p - \omega_s = \omega_{vib}$ where a *single* vibrational level is excited. Multiplex CARS can also be achieved by using spectrally broader (fs) Stokes pulses to excite *multiple* bands of vibrational levels and identify them by measuring the spectrally resolved anti-Stokes photons.

CARS is typically challenging to implement due to the strict spatiotemporal overlap requirement of several beams from several sources.^{11–13} To overcome this issue, single-beam techniques have been developed using shaped, spectrally broad femtosecond pulses to simultaneously provide the necessary pump, Stokes, and probe photons.^{14–17} By employing single-beam techniques, spatiotemporal overlap is inherently achieved; however, the exclusive use of temporally short, femtosecond pulses results in a nonresonant four-wave mixing (FWM) signal that is orders of magnitude greater than the resonant CARS signal.^{15,16} The measured CARS signal is, therefore, the coherent sum of the resonant and nonresonant signals, as shown in Eq. (1).

A variety of CARS schemes have been developed in order to suppress the nonresonant background signal, such as tailoring the temporal width and delay of the probe-pulse,¹⁰ using polarization pulse shaping techniques,^{4,8} and employing coherent control.¹⁴ These schemes exploit different properties of the nonlinear FWM interaction to achieve the goal of background-free measurements. While these methods are effective for applications such as microscopy,^{14,18} they are

not necessarily suitable for long-range standoff probing of scattering samples. Under such conditions, polarization shaping is sensitive to the depolarization caused by the multiple random scattering in the sample. Furthermore, the nonresonant signal can serve to amplify the resonant signal and, thus, suppression can result in a remaining resonant signal that is too weak to be detected.

In this work, we demonstrate single beam standoff detection of traces of solids without using a complex pulse shaping apparatus or nonresonant background suppression. Instead, we use a commercially available notch filter as passive optical element and exploit the nonresonant signal in a homodyne amplification scheme.

For the notch filter, we use a resonant photonic crystal slab (RPCS), which is a waveguide etched with a subwavelength grating that creates a tunable notch feature in the spectrum (Figs. 1(a) and 1(b)). The notch can be adjusted over a wide spectral range by changing its angle with respect to the incident beam.¹⁹ The use of an RPCS as a passive shaping element has been recently demonstrated in single-pulse CARS micro-spectroscopy.²⁰ In this technique, the spectral notch feature serves as a narrow probe that allows for multiplex CARS detection. We exploit the strong nonresonant background and use it as a local oscillator in a homodyne amplification scheme:

$$I(\omega) = |P^{NR}(\omega) + P^R(\omega)|^2 \\ \simeq |P^{NR}(\omega)|^2 + 2|P^R(\omega)||P^{NR}(\omega)|\cos\phi(\omega), \quad (1)$$

where $I(\omega)$ is the measured signal intensity at frequency ω , P^R , and P^{NR} are the resonant and nonresonant signals, respectively, and ϕ is the relative spectral phase between them. Usually, with ultrashort pulses $|P^{NR}(\omega)|^2 \gg |P^R(\omega)|^2$, making the resonant signal challenging to measure.^{10,15,16}

However, the cross term is the product of a strong, smooth, and featureless nonresonant signal, with a weak resonant signal that has a typical spectral phase modulation around a vibrational resonance. The phase modulation is governed by the vibrational resonance lineshape and the phase structure of the RPCS notch resonance.¹⁵ As a result, the resonant feature is amplified by several orders of magnitude, allowing detection of the much weaker coherent Raman signal.

To demonstrate the ability to remotely detected back-scattered CARS signal, we probed samples with 30 fs pulses

^{a)}Author to whom correspondence should be addressed. Electronic mail: natan@stanford.edu.

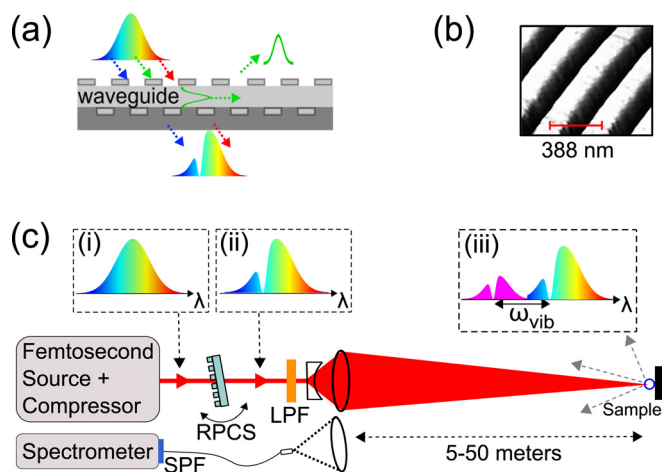


FIG. 1. (Color online) (a) Schematic diagram of the RPCS filter. (b) AFM image of the RPCS surface (from Thayil *et al.*, *Optics Express* **16**(17), 13315 (2008). Copyright © 2008). Reproduced with permission, © 2012 Optical Society of America. (c) The experimental setup. The broadband excitation pulse (i) is shaped with a tunable narrowband spectral notch by the RPCS filter (ii). A long-pass filter (LPF) is then used to attenuate the short-wavelength region. The spectral notch serves as a probe for the CARS process, generating narrow features which are blue-shifted from the probe by the vibrational frequencies (iii). The scattered light is collected, then short-pass filtered (SPF) and coupled to a spectrometer.

(Femtolasers GmbH) that were notch filtered by an RPCS filter. The pulses were then long-pass filtered around the spectral region that overlapped with the CARS signal, and focused on samples at distances of 5–50 m (Fig. 1(c)). The beam diameter on the sample was ≈ 1.5 mm, resulting in peak powers of $\approx 10^{11}$ W/cm². We collected the backscattered CARS signal from various materials using a single 7.5 in. lens imaging configuration. The light was then short-pass filtered and fiber coupled to a spectrometer (Horiba Jobin Ivon, Triax 321). We placed a black absorptive material behind the samples to eliminate the possibility of collecting specular reflections of the much stronger forward CARS signal. This is in contrast to previous studies that placed the sample on a reflective surface,⁸ while assuming the worst-case scenario for real-life situations, where a minute contribution to the signal due to diffusive reflections from the background material will occur. Such contribution can be estimated by $\rho D^2/16r^2$, with background reflectivity ρ , collecting lens diameter D at distance r from the sample, yielding an attenuation of at least 10^{-7} for the setup used. For each acquisition, we obtained two measurements, corresponding to different notch positions, spectrally separated by the notch width (≈ 1 nm). The CARS spectra were obtained with integration times ranging from 1 to 5 s. The typical signal power collected by the spectrometer was ≈ 1 pW. The dispersion induced by the propagation in air was compensated using the internal prism compressor of the laser source.

Typical CARS spectra from complimentary notch locations are shown in Fig. 2. The interference feature due to the resonant contribution at 1051 cm^{-1} is evident in the KNO_3 spectrum. In order to extract the Raman line, we normalized the differential measurement by P^{NR} (Ref. 20)

$$I_{CARS}(\omega) \propto \frac{I_n(\lambda+\Delta\lambda)(\omega)}{P_{n(\lambda+\Delta\lambda)}^{NR}(\omega)} - \frac{I_n(\lambda)(\omega)}{P_{n(\lambda)}^{NR}(\omega)}, \quad (2)$$

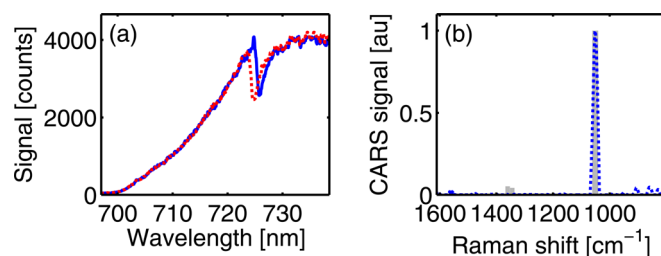


FIG. 2. (Color online) (a) Raw spectra of trace amount (<1 mg) of KNO_3 collected from a distance of 5 m, using two notch positions: 784 nm (dashed line) and 785 nm (solid line) with integration time of 3 s. (b) Taking the normalized difference of the two spectra by the non-resonant spectra (dashed line), the Raman line (solid line) is retrieved.

where $I_n(\lambda)$ is the intensity measured with a notch at wavelength λ , of width $\Delta\lambda$, and P^{NR} is approximated by smoothing $\sqrt{I_n(\lambda)(\omega)}$ using a moving average filter with 1 nm window following a median filter with 3 nm window. We have found that estimating P^{NR} for each notch acquisition helps reduce beam pointing fluctuations effects between the two acquisitions.

Experimentally resolved Raman spectra of traces of solids and explosives particles are presented in Fig. 3. The measured spectra are in a good agreement with the known Raman lines of the probed materials.⁹ In our experiments, the acquisition time was limited by the beam-point stability of the experimental setup. For example, the missing Raman lines in Fig. 3(a) were detectable in shorter distances (not shown); however, the limited beam pointing stability and the available laser bandwidth obscure them at longer distances. Actively stabilizing the beam would reduce signal fluctuations between measurements and allow shorter measurement times. Other alternative shaping techniques could also be used to generate a similar spectral notch-like feature. For example, the use of an interference filter, Fabry-Perot interferometer, or fiber Bragg grating would yield similar results.

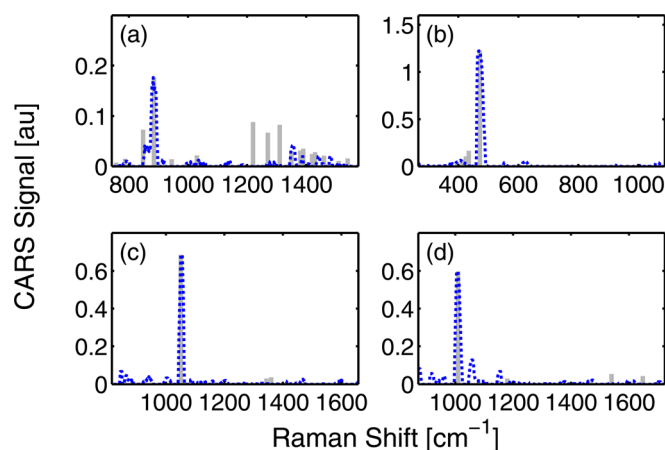


FIG. 3. (Color online) Resolved CARS spectra of several scattering samples (dashed line). (a) Cyclotrimethylene-trinitramine (RDX/T4) <1 mg (b) sulfur powder $<500\ \mu\text{g}$ (c) crystallized potassium nitrate (KNO_3) <1 mg (d) crystallized urea <4 mg. Spectra were obtained at a standoff distances of (a) 24 m and (b-d) 50 m, with integration times of (a) 3 s (b) 5 s (c) 5 s (d) 1 s. The samples have glass like morphology. The Raman lines (solid line) are plotted for reference.

However, these lack the simplicity, compactness, and compatibility with high intensities.

Femtosecond CARS spectroscopy using a spectral notch filter has numerous advantages over other single beam techniques. The RPCS is virtually alignment free and has broad tunability allowing for flexibility in the detection window, while nearly eliminating the inherent losses of grating based pulse shapers. A transmission of almost unity is particularly beneficial as the CARS signals are cubically proportional to the pulse intensity. Moreover, the RPCS can be mounted on a galvanometric mirror to achieve rapid (KHz) modulation rates that are 1.5 orders of magnitude faster than typical liquid crystal spatial light modulators (LC-SLMs) allowing lock-in detection and fast scanning. Additional signal enhancement can be made using multiple notch filters. By spectral positioning of several notches spaced by the vibrational lines of a known substance, the coherent addition of signals from several vibrational levels will generate a feature, which is significantly larger than the linear sum of the individual contributions.²¹

We thank S. Soria for providing the RPCS filter and the AFM image used in this work.¹⁹ We also thank E. Grinvald, G. Elazar, and G. Han for invaluable help. This work was supported in parts by DHS Center of Excellence of Explosives Detection, Mitigation, Response and by NATO Project No. SfP-983789. J.M.L. was supported by the European MC-ITN FASTQUAST.

¹National Research Council, Committee on the Review of Existing and Potential Standoff Explosives Detection Techniques, *Existing and Potential Standoff Explosives Detection Techniques* (National Academies, Washington, DC, 2004).

- ²S. Wallin, A. Pettersson, H. Östmark, and A. Hobro, *Anal. Bioanal. Chem.* **395**, 259 (2009).
- ³P. R. Hemmer, R. B. Milesb, P. Polynkinc, T. Sieberta, A. V. Sokolova, P. Spranglee, and M. O. Scully, *Proc. Natl. Acad. Sci. U.S.A.* **108**, 3130 (2011).
- ⁴M. T. Bremer, P. J. Wrzesinski, N. Butcher, V. V. Lozovoy, and M. Dantus, *Appl. Phys. Lett.* **99**, 101109 (2011).
- ⁵A. Portnov, S. Rosenwaks, and I. Bar, *Appl. Phys. Lett.* **93**, 041115 (2008).
- ⁶J. C. Carter, S. M. Angel, M. Lawrence-Snyder, J. Scaffidi, R. E. Whipple, and J. G. Reynolds, *Appl. Spectrosc.* **59**, 6 (2005).
- ⁷D. Pestov, X. Wang, G. O. Ariunbold, R. K. Murawski, V. A. Sautenkov, A. Dogariu, A. V. Sokolov, and M. O. Scully, *Proc. Natl. Acad. Sci. U.S.A.* **105**, 2 (2008).
- ⁸H. Li, D. A. Harris, B. Xu, P. J. Wrzesinski, V. V. Lozovoy, and M. Dantus, *Opt. Express* **16**, 5499 (2008).
- ⁹O. Katz, A. Natan, Y. Silberberg, and S. Rosenwaks, *Appl. Phys. Lett.* **92**(17), 171116 (2008).
- ¹⁰D. Pestov, R. K. Murawski, G. O. Ariunbold, X. Wang, M. Zhi, A. V. Sokolov, V. A. Sautenkov, Y. V. Rostovtsev, A. Dogariu, Y. Huang *et al.*, *Science* **316**, 265 (2007).
- ¹¹B. Schrader, *Infrared and Raman Spectroscopy* (VCH, Weinheim, 1995).
- ¹²A. Volkmer, *J. Phys. D: Appl. Phys.* **38**, R59 (2005).
- ¹³C. L. Evans and S. X. Xie, *Annu. Rev. Anal. Chem.* **1**(1), 883 (2008).
- ¹⁴N. Dudovich, D. Oron, and Y. Silberberg, *Nature* **418**(6897), 512 (2002).
- ¹⁵D. Oron, N. Dudovich, and Y. Silberberg, *Phys. Rev. Lett.* **89**(27), 273001 (2002).
- ¹⁶S. H. Lim, A. G. Caster, and S. R. Leone, *Opt. Lett.* **32**, 10 (2007).
- ¹⁷C. Müller, B. Tiago, B. von Vacano, and M. Motzkus, *J. Raman Spectrosc.* **40**, 809 (2009).
- ¹⁸X. S. Xie, J. Yu, and W. Y. Yang, *Science* **312**, 228 (2006).
- ¹⁹A. Thayil, A. Muriano, J. P. Salvador, R. Galve, M. P. Marco, D. Zalvidea, P. Loza-Alvarez, T. Katchalski, E. Grinvald, A. A. Friesem *et al.*, *Opt. Express* **16**(17), 13315 (2008).
- ²⁰O. Katz, J. M. Levitt, E. Grinvald, and Y. Silberberg, *Opt. Express* **18**, 22693 (2010).
- ²¹D. Oron, N. Dudovich, and Y. Silberberg, *Phys. Rev. A* **70**, 023415 (2004).